

# Optical Characterization of Oxide Encapsulated Silicon Nanowires of Various Morphologies

Sharon M. King<sup>1,\*</sup>, Shweta Chaur<sup>1,†</sup>, Sathesh Krishnamurthy<sup>1,\*</sup>,  
Werner J. Blau<sup>1</sup>, Alan Colli<sup>2</sup>, and Andrea C. Ferrari<sup>2</sup>

<sup>1</sup>*School of Physics, Trinity College Dublin, Dublin 2, Ireland*

<sup>2</sup>*Centre for Advanced Photonics and Electronics, University of Cambridge, Cambridge CB3 0FA, UK*

The optical properties of four different silicon nanowire structures were investigated. Two of the samples consisted of spheres of nanocrystalline silicon encapsulated by silicon oxide nanowires, with other two consisting of crystalline silicon nanowires coated by silicon oxide shells. The nanostructures produced by oxide assisted growth consisted of spheres of crystalline silicon encapsulated by silicon oxide shells. The absorption and photoluminescence of the different structures of the sample are investigated. The emitting species responsible for photoluminescence across the visible spectrum are discussed. Thu, 17 Jul 2008 13:44:24

**Keywords:** Si Nanowires, Nanostructures, Quantum Confinement, Defects, Excitons, Photoluminescence, Ageing.

## 1. INTRODUCTION

The miniaturisation of silicon based electronics has fuelled interest in nanoelectronics.<sup>1</sup> Silicon nanostructures are promising components for use in nanoscale devices. This is partly due to the controllability of their growth, which enables the tailored production of nanostructures. Promising biological and chemical sensor applications of silicon nanostructures are under investigation,<sup>2</sup> as well as silicon nanowire based devices<sup>3,4</sup> such as nanowire transistors.<sup>4</sup> Extensive research has been carried out on understanding the origin of light emission in silicon nanowires.<sup>1,5</sup> The proposed origins include, the existence of excess silicon atoms in the silicon nanostructures;<sup>6</sup> defect centres in the silicon oxide layer that surrounds the nanowires;<sup>7</sup> and in the case of chainlike nanowires that incorporate spheres of crystalline silicon into the structure, defects in the silicon oxide and/or the interface between silicon oxide and the nanoparticles.<sup>5</sup> The motivation of this study is to investigate the PL spectra produced by silicon nanowires of various morphologies, and to ascertain the origin of the emitting species. Some basic optical characterization has been carried out on similar nanostructures,<sup>8</sup> but this work

has not been extensive. This report comprises a comprehensive investigation of the materials, including structural, absorption and PL characterization.

## 2. EXPERIMENTAL DETAILS

### 2.1. Materials

Two of the wire structures consisted of spheres of crystalline silicon encapsulated by silicon oxide. The other two samples consisted of crystalline silicon nanowires with silicon oxide outer shells. Samples A and B were produced by an oxide assisted growth process.<sup>8</sup> The oxide assisted growth process involves the evaporation of SiO powder under argon flow in a high temperature furnace. The wires were collected on a quartz support positioned in the 900–950 °C region of the furnace tube. The total argon pressure during the process determined the sample morphology. Sample C was prepared by a gold catalyzed thermal evaporation method, where the silicon vapour was provided by thermal evaporation of pure silicon powder. The process was carried out at 700–800 °C.<sup>8</sup> Sample D was produced by chemical vapour deposition (CVD) with SiH<sub>4</sub> as precursor and Au as catalyst.<sup>9</sup>

### 2.2. Structural Characterization

Figure 1 shows transmission electron microscopy (TEM) images of the different wire morphologies that were

\*Authors to whom correspondence should be addressed.

†Present address: Materials Department, Queen Mary College, University of London, UK.

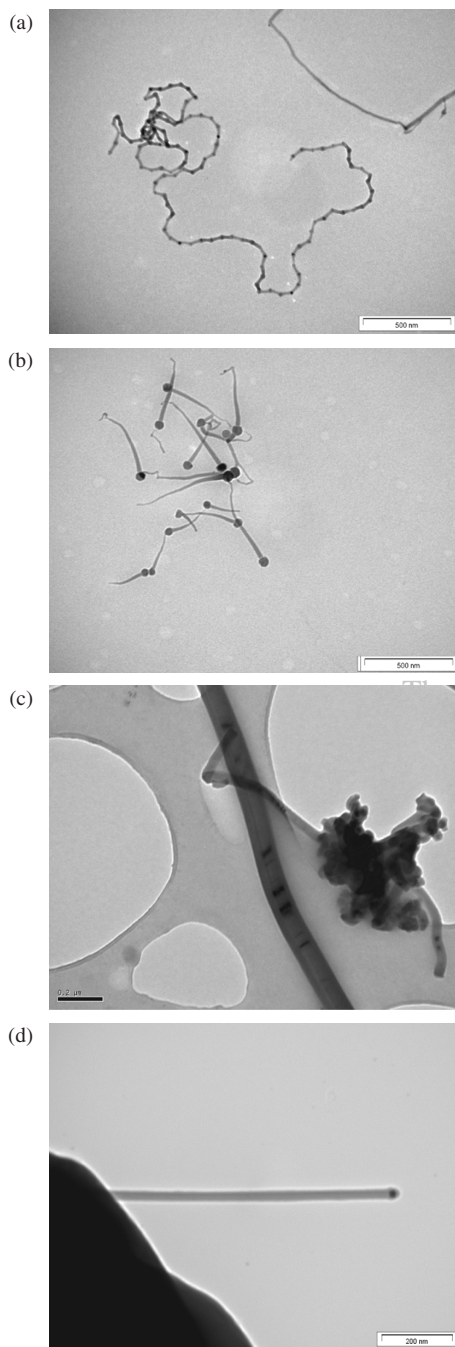


**Fig. 1.** TEM study of nanostructures. Samples A and B contain spheres of crystalline silicon encapsulated by silicon oxide. Sample A is a chain-like structure and Sample B is a tadpole-like structure. Samples C and D have a similar morphology, but were grown by different methods. They consist of crystalline silicon nanowires encapsulated by silicon oxide.

investigated. The samples were prepared on 400 mesh holey carbon grids, using a drop casting deposition method from isopropanol (IPA) solution. A Hitachi H-7000 TEM was used to obtain the images. Figure 1(a) shows Sample A, which had a chain-like structure. It consisted of crystalline Si balls approximately 20 nm in diameter, surrounded and connected by SiO<sub>2</sub> shells. Figure 1(b)

**Table I.** Information regarding sample morphology.

Name	Morphology	Si wire core/sphere diameter
Sample A	Chain-like	20 nm-sphere
Sample B	Tadpole-like	70 nm-sphere
Sample C	Straight	40 nm-wire
Sample D	Straight	38 nm-wire

depicts the morphology of Sample B, which consisted of a ball and wire structure. The balls were approximately 70 nm in diameter, were highly crystalline, as were the cores of the wires. A relatively thick oxide shell (5–10 nm) was found on the ball and wire structures. Figure 1(c) shows Sample C, which consists of straight silicon nanowires with a crystalline core approximately 40 nm in diameter, and over-coated in oxide. The wire in the image shown has a larger diameter than the average wire in Sample C, but is included in this report as it provides a good detailed image of the structure. Figure 1(d) is of Sample D. It consisted of straight silicon nanowires with a crystalline core approximately 38 nm in diameter, and over-coated in oxide. Table I displays information regarding the morphology of each sample.

### 2.3. Optical Characterization

Optical characterization was carried out on the samples in IPA solution. The wires were first dispersed in spectroscopic grade IPA under agitation by a sonic tip. To ensure that the concentration of the solution would not change during the investigation process due to sedimentation, a stable suspension of each sample was obtained. This was achieved by determining the sedimentation profiles of the wire samples.<sup>10</sup> The samples were then left to stand while the unstable phases separated out, and the relatively stable components of the suspensions were then pipetted off. The “stable” phases were very good dispersions which would eventually undergo sedimentation if left to stand for weeks or months. The optical characterization was carried out on these stable phases. The stability of the dispersions ensured that the concentrations of the solutions were not changing during the investigation process. The “unstable” phases which were separated out consisted of bundles of nanowires.

## 3. RESULTS AND DISCUSSION

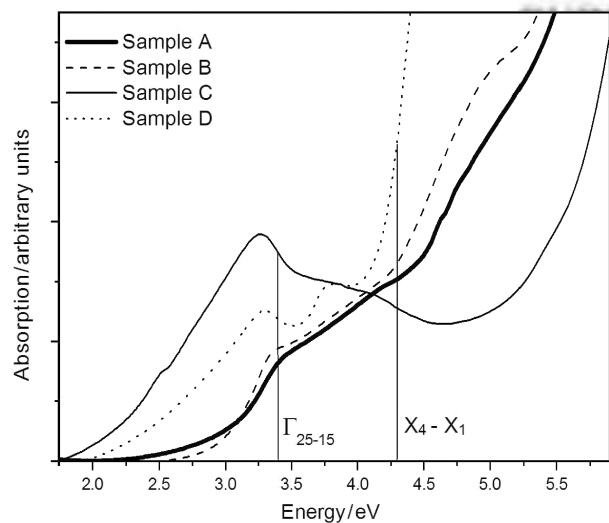
### 3.1. Absorption Spectroscopy

Figure 2 shows the absorption spectra of all the samples. Experiments were performed using a Shimadzu absorption spectrometer. All of the samples display shoulders near the direct band-gap energies of bulk crystalline silicon;<sup>11,12</sup> with the absorption being dominated by direct transitions. Samples A and B show a peak in absorption at 3.4 eV.

The shoulder in absorption for Sample B does extend out to 3.34 eV, and may be evidence of weak quantum confinement effects. Quantum confinement is expected to influence the  $\Gamma_{25}-\Gamma_{15}$  (3.4 eV) direct transition.<sup>13</sup> Red-shift of the  $\Gamma_{25}-\Gamma_{15}$  is attributed to quantum confinement. Holmes reported a red-shift for crystals approximately 2 nm in diameter.<sup>14</sup> Rama Krishna and Friesner also predict red-shift of  $\Gamma_{25}-\Gamma_{15}$  with decreasing nanocluster size.<sup>15</sup> Samples C and D both display red-shifted  $\Gamma_{25}-\Gamma_{15}$  absorption peaks. Sample C shows a 0.14 eV red-shift, and Sample D a 0.1 eV red-shift. Quantum confinement cannot be occurring in the large crystalline spheres in Samples A and B, or in the wide nanowires in Samples C and D. Quantum confined features may be resulting from small nanocrystals which are preferentially formed at the  $\text{SiO}_x/\text{Si}$  interface due to nucleation kinetics. The red-shift is most apparent for the samples which contain crystalline nanowire cores, i.e., Samples C and D, and some weak quantum confined effects may be occurring in Sample B, which contains crystalline silicon nanowires attached to spheres of silicon. Hence the absorption at the  $\Gamma_{25}-\Gamma_{15}$  transition implies that small nanocrystals may be preferentially formed at the  $\text{SiO}_x/\text{Si}$  interface in straight silicon nanowires.

Samples A and B exhibit a strong increase in absorption above the  $X_4-X_1$  (4.3 eV) direct transition. Sample C exhibits a broad shoulder in the  $X_4-X_1$  region, and weak absorption compared to that in the region of the  $\Gamma_{25}-\Gamma_{15}$  transition. Sample D exhibits a prominent shoulder at 3.8 eV, and strong absorption at 4.3 eV.

In summary, Samples A and B exhibit an absorption shoulder at the  $\Gamma_{25}-\Gamma_{15}$  point, and a strong absorption onset at the  $X_4-X_1$  transition energy. Samples C and D clearly exhibit quantum confined features. They undergo a red-shift of the  $\Gamma_{25}-\Gamma_{15}$  transition, which is



**Fig. 2.** Optical absorption. The absorption is dominated by direct transitions at the  $\Gamma_{25}-\Gamma_{15}$  and  $X_4-X_1$  points. There are also features characteristic of quantum confinement.

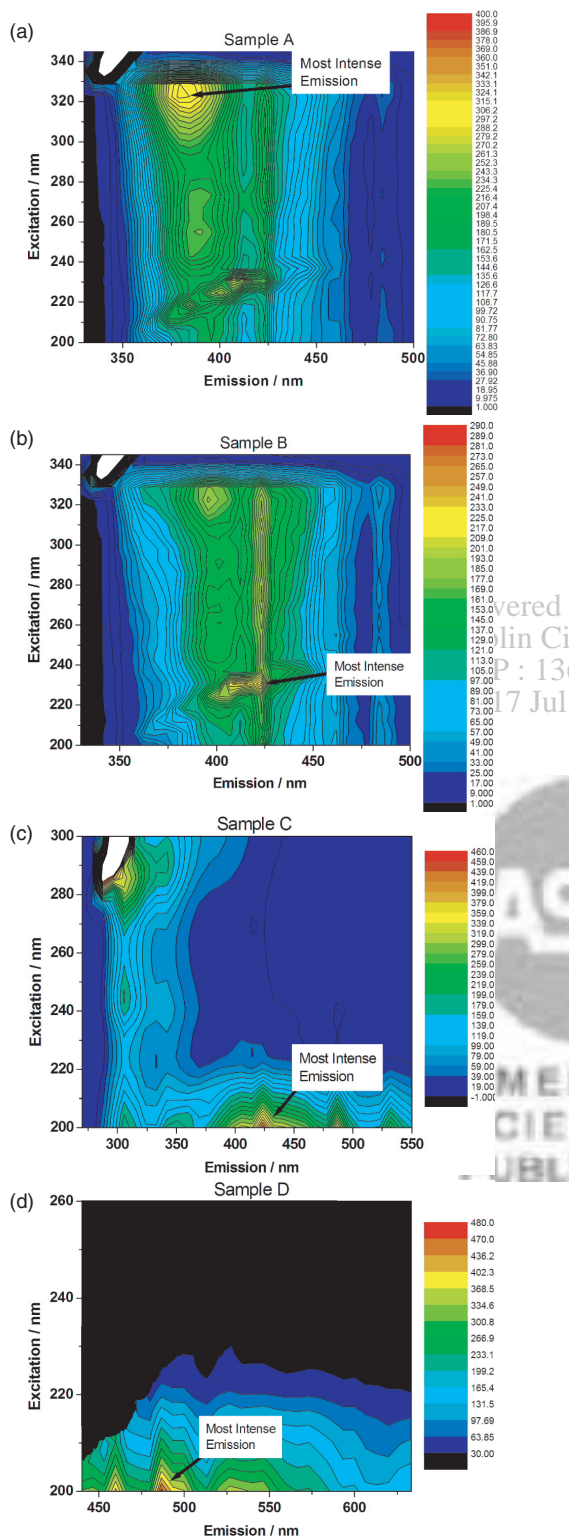
indicative of quantum confinement from the presence of small crystallites.

### 3.2. Photoluminescence Spectroscopy

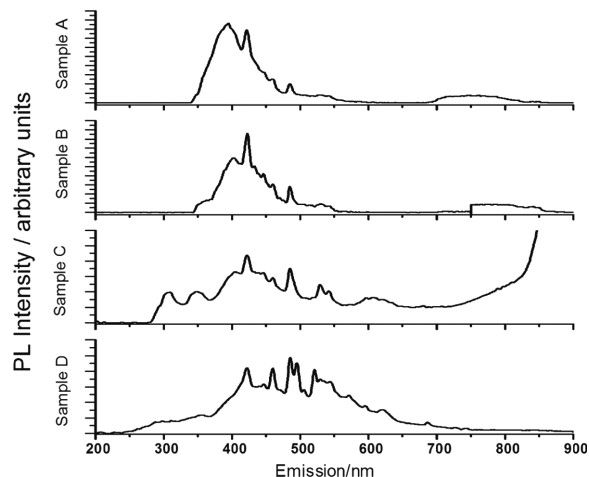
A three dimensional (3D) PL study was performed on the samples, see Figure 3. Samples A [Fig. 3(a)] and B [Fig. 3(b)] produced PL for excitation wavelengths between 200 and 345 nm. Sample A's most intense emission peak occurred at 384 nm, for an excitation wavelength of 323 nm. Sample B shows a strong emission peak at 400 nm when excited at 323 nm, but it's most intense peak in emission occurred at 423 nm, for a corresponding excitation wavelength of 231 nm. Evidence of an inhomogeneous size distribution can be seen from the ridge-like structure that occurs across the 3D PL graphs. Sample C emitted for excitation wavelengths between 200 and 320 nm [Fig. 3(c)], although not as strongly as Samples A and B. Sample D only emitted for excitation wavelengths between 200 and 230 nm [Fig. 3(d)]. Samples C and D appear to have very similar morphologies [Figs. 1(c), (d) and 2]. Sample C was produced by a gold catalyzed thermal evaporation method, whereas Sample D was produced by a CVD process. It is possible that the production method as well as the final morphology of the sample dictates the effective band-structure of the nanowire. A high resolution transmission electron microscopic study of the samples would elucidate the issue and is a promising technique for future research.

Figure 4 shows the PL of the nanostructures for excitation at 200 nm. Intense PL occurs for Sample C between 800 nm and 900 nm. PL in this region has been attributed to a combination of defects and strain.<sup>16</sup> PL occurs in the red region (700–800 nm) for all samples. The luminescence in this region is attributed to radiative recombination of carriers in silicon nanocrystallites formed at the  $\text{SiO}_x/\text{Si}$  interface.<sup>17</sup> Small nanocrystals are preferentially formed in this region due to nucleation kinetics. The variation in local optical density of states along the wire affects the PL emission intensity. It is also expected to influence the spontaneous emission rate of silicon nanocrystals. We attribute emission in the yellow region (500–600 nm) to radiative decay of self trapped excitons at the  $\text{SiO}_x/\text{Si}$  interface. A study of the yellow PL from silicon crystallites in thermally grown silicon dioxide thin films indicates that the self trapped excitons are confined to oxygen sufficient structures such as  $\text{SiO}_3$  or  $\text{SiO}_4$ .<sup>18</sup> Samples A and B photo-luminesce weakly in the 500–600 nm region, whereas Samples C and D produce strong emission in this region. This would suggest that oxygen sufficient centres are preferentially forming along the  $\text{SiO}_2/\text{Si}$  interface of the straight nanowires.

The dominant emission for Samples A and B occurs in the ultra-violet to violet region (350–450 nm). It is likely that the PL arises from direct recombination of carriers at the interface between the crystalline silicon



**Fig. 3.** 3D PL study. Excitation wavelength is displayed on the Y-axis, and emission wavelength on the X-axis. PL intensity varies from blue (weak) to red (intense). The position of the most intense emission for each sample is marked on the graphs. Sample C [Fig. 3(c)] actually emits most intensely in the red region, but the 3D representation is confined to the violet-green region, as most of the interesting features occur in this region. PL of each sample in the region 200–900 nm is displayed in Figure 4.



**Fig. 4.** PL of each sample when excited at 200 nm.

nanoclusters and the oxide shell. The radiative lifetime for emission at 420 nm for Sample A was investigated. For the PL lifetime investigation, ultra-pure water was used as the solvent. The PL decay was best fit by a three exponential decay. Three nanosecond-scale lifetimes were recorded. This rapid decay is indicative of direct band gap recombination. PL also occurs for Samples C and D in this region, but it is not the most intense emission region for either of these two samples. The spherical nature of the large silicon nanoclusters in Samples A and B may be the reason for 350–450 nm being the dominant PL region for these samples. Increased vibronic coupling between the crystalline silicon and the highly ionic  $\text{SiO}_2$  (Ref. [19]) would be possible due to the spherical nature of the nanoparticles which allows for increased contact between the crystalline spheres and the terminating surface. It has been shown that chainlike (silicon oxide embedded nanocrystals) nanowires exhibit a much stronger  $\text{SiO}_2$  resonance in X-ray absorption than standard silicon nanowires. This has been attributed to a larger ratio of silicon oxide atoms to elemental silicon atoms in the chainlike wires.<sup>5</sup>

PL occurred at wavelengths close to the  $\Gamma_{25}-\Gamma_{15}$  (3.4 eV) direct energy gap of bulk silicon.<sup>11,12</sup> All of the samples displayed features, varying in prominence from small shoulders (Sample A) to large peaks (Sample C), at 349 nm (3.55 eV). This corresponds to direct electron hole recombination at the  $\Gamma_{25}-\Gamma_{15}$  point. A major PL peak centered at 3.4 eV for has been reported for silicon nanoclusters by other groups, and was attributed to direct recombination at  $\Gamma_{25}-\Gamma_{15}$ .<sup>13</sup> The  $\Gamma_{25}-\Gamma_{15}$  transition in our samples is blue shifted, which is consistent with an increase in excitonic recombination energy due to an oxidation induced size reduction.<sup>20</sup>

#### 4. SUMMARY

The PL of silicon nanowire structures grown by a variety of methods was investigated. The samples displayed some

absorption features which were characteristic of quantum confinement. For silicon nanowires with crystalline cores (Samples C and D), the quantum confined features were observable at the  $\Gamma_{25}-\Gamma_{15}$  transition. PL occurred across the visible region for all of the samples under investigation. The PL produced by each sample was indicative of the production method and the final sample morphology. PL in the red region (700–800 nm) is attributed to radiative recombination of carriers in silicon nanocrystallites formed at the  $\text{SiO}_x/\text{Si}$  interface. Emission in the yellow (500–600 nm) region is attributed to radiative decay of self trapped excitons at the  $\text{SiO}_x/\text{Si}$  interface. This is the dominant emission region for Samples C and D. The dominant emission for Samples A and B occurred in the ultra-violet to violet region (350–450 nm). This emission is attributed to direct recombination of carriers at the interface between the crystalline silicon nanoclusters and the oxide shell.

**Acknowledgments:** This work was supported by Science Foundation Ireland. Many thanks to Dr. Hugh J. Byrne at the Focas Institute, Dublin Institute of Technology and Dr. Alan G. Ryder at the National University of Ireland-Galway, for arranging the PL lifetime study.

## References and Notes

1. Y. Cui and C. M. Lieber, *Science* 291, 851 (2001).
2. Y. Cui, Q. Wei, H. Park, and C. M. Lieber, *Science* 293, 1289 (2001).
3. S. Chung, J. Yu, and J. R. Heath, *Appl. Phys. Lett.* 76, 2068 (2000).
4. L. T. Canham, T. I. Cox, A. Loni, and A. J. Simons, *Applied Surface Science International Symposium on Si Heterostructures*, September (1996), Vol. 102, p. 436.
5. X. H. Sun, N. B. Wong, C. P. Li, S. T. Lee, and T. K. Sham, *J. Appl. Phys.* 96, 3447 (2004).
6. X. L. Wu, S. J. Xiong, G. G. Siu, G. S. Huang, Y. F. Mei, Z. Y. Zhang, S. S. Deng, and C. Tan, *Phys. Rev. Lett.* 91, 157402 (2003).
7. Jifa Qi, J. M. White, A. M. Belcher, and Y. Masumoto, *Chem. Phys. Lett.* 372, 763 (2003).
8. A. Colli, S. Hofmann, A. Fasoli, A. C. Ferrari, C. Ducati, R. E. Dunin-Borkowski, and J. Robertson, *J. Appl. Phys.* A 85, 247 (2006).
9. S. Hofmann, C. Ducati, R. J. Neill, S. Piscanec, A. C. Ferrari, J. Geng, R. E. Dunin-Borkowski, and J. Robertson, *J. Appl. Phys.* 94, 6005 (2003).
10. V. Nicolosi, D. Vrbancic, A. Mrzel, J. McCauley, S. O'Flaherty, C. McGuinness, G. Compagnini, D. Mihailovic, W. Blau, and J. Coleman, *J. Phys. Chem. B* 109, 7124 (2005).
11. J. Singleton, *Band Theory and Electronic Properties of Solids*, Oxford University Press, Great Clarendon Street, Oxford, U.K. (2001).
12. M. Fox, *Optical Properties of Solids*, Oxford University Press, Great Clarendon Street, Oxford, U.K. (2001).
13. J. P. Wilcoxon, G. A. Samara, and P. N. Provencio, *Phys. Rev. B* 60, 2704 (1999).
14. J. D. Holmes, K. J. Ziegler, R. C. Doty, L. E. Pell, K. P. Johnston, and B. A. Korgel, *J. Am. Chem. Soc.* 123, 3743 (2001).
15. M. V. Rama Krishna and R. A. Friesner, *J. Chem. Phys.* 96, 873 (1992).
16. X. B. Zeng, X. B. Liao, B. Wang, S. T. Dai, Y. Y. Xu, X. B. Xiang, Z. H. Hu, H. W. Diao, and G. L. Kong, *J. Cryst. Growth* 265, 94 (2004).
17. K. S. Zhuravlev, I. E. Tyschenko, E. N. Vandyshev, N. V. Bulytova, A. Misiuk, L. Rebohle, and W. Skorupa, *Siberian Russian Workshop on Electron Devices and Materials Proceedings* (2002), pp. 1–5.
18. W. C. Choi, M. Lee, E. K. Kim, C. K. Kim, S. Min, C. Park, and J. Y. Lee, *Appl. Phys. Lett.* 69, 3402 (1996).
19. O. Engstrom and H. G. Grimmeiss, *Semicond. Sci. Technol.* 4, 1106 (1989).
20. Y. Kanemitsu, *J. Lumin.* 100, 209 (2002).

Received: 7 January 2007. Accepted: 7 January 2007.